Does the Like Dissolves Like Rule Hold for Fullerene and Ionic Liquids?

Vitaly V. Chaban · Cleiton Maciel · Eudes Eterno Fileti

Abstract Over 150 solvents have been probed to dissolve light fullerenes, but with a quite moderate success. We uncover unusual mutual polarizability of C_{60} fullerene and selected room-temperature ionic liquids, which can be applied in numerous applications, e.g. to significantly promote solubility/miscibility of the highly hydrophobic C_{60} molecule. We report electron density and molecular dynamics analysis supported by the state-of-the-art hybrid density functional theory and empirical simulations with a specifically refined potential. The analysis suggests the workability of the proposed scheme and opens a new direction to obtain well-dispersed fullerene containing systems. A range of common molecular solvents and novel ionic solvents are compared to 1-butyl-3-methylimidazolium tetrafluoroborate.

Keywords Fullerene · Buckyball · Ionic liquid · Solvation · Electronic structure · Molecular dynamics

1 Introduction

Efficient dissolution of fullerenes is an old quest started in 1985 [1]. Fullerene solutions are important for numerous applications including, but not limited to, development of cosmetic products, robust drug delivery, extraction and separation of nanostructures from industrial

V. V. Chaban (✉)
MEMPHYS - Center for Biomembrane Physics, University of Southern Denmark, 5230 Odense M, Denmark
e-mail: vvchaban@gmail.com; chaban@sdu.dk

C. Maciel
Centro de Ciências Naturais e Humanas, Universidade Federal do ABC, Santo André, SP 09210-270, Brazil

E. E. Fileti
Instituto de Ciência e Tecnologia, Universidade Federal de São Paulo, 12231-280 São José dos Campos, SP, Brazil

soot, photovoltaics, investigation of chemical reactions involving fullerenes, etc. [2–10] Solutions and colloidal systems of fullerenes belong to one of the most studied systems in modern chemistry. A variety of solvents (over 150) and their mixtures were applied to obtain real solutions of C_{60}, C_{70}, and some higher fullerenes [4, 11, 12]. The available data are, however, rather pessimistic. In the majority of polar solvents, including water, solutions of fullerenes are either extremely diluted or colloidal ones [4]. Relatively concentrated solutions are achieved in some solvents of low polarity, such as aromatic hydrocarbons and their haloderivatives. For instance, solubility of C_{60} in benzene equals 1.50 g·L^{-1} [13], 2.40 g·L^{-1} in toluene [14], and 2.60 g·L^{-1} in ethylbenzene [13], all measurements being done at 298 K. Remarkably, methylation of the solvent molecule significantly increases its affinity to C_{60}, although the chemical background of this empirical finding is unclear. 1,2,3-Trimethylbenzene allows for solubility increase by more than three times, compared to benzene, up to 4.70 g·L^{-1} [15]. The same authors reported 17.90 g·L^{-1} for 1,2,4-trimethylbenzene and 5.80 g·L^{-1} for 1,2,3,4-tetramethylbenzene [15], although the first quantity looks doubtful to us. Halogenation of low molecular aromatic compounds provides even better results in many cases: 6.35 in chlorobenzene, 13.80 in 1,2-dibromobenzene, 9.62 in 1,2,4-trichlorobenzene, etc. [12]. Grafting other functional groups does not lead to comparable effects. Benzonitrile, nitrobenzene, phenyl isocyanate, n-propylbenzene, n-butylbenzene and a few other solvents, carefully summarized by Semenov et al. [11, 12], are notably unsuccessful for pristine light fullerenes.

The highest solubility of C_{60} that we are aware of was achieved by Talukdar and coworkers [14], who used piperidine (53.28 g·L^{-1}) and pyrrolidine (47.52 g·L^{-1}). It was hypothesized that these solvents exhibited specific donor–acceptor interactions with C_{60}, C_{70}, C_{84}, and C_{100} that can, under certain conditions, give rise to formation of new chemical compounds. Piperidine and pyrrolidine are sometimes called "reactive" solvents with respect to C_{60}. Note, that published references on solubility contain lots of contradicting results. This fact can be correlated with specific methods of measurements, their internal uncertainties, and preparation of fullerene containing solutions [4, 12, 16–18]. In all polar and many low-polarity solvents, fullerenes tend to form colloidal systems, being another source of the scattered, ambiguous results.

Apart from direct experiments outlined above, numerous computer simulations have been conducted on fullerenes in solutions [19–22]. Monticelli and coworkers published a few important developments in atomistic and coarse-grained force fields [19, 23, 24]. One of us reported free energies and structure patterns of C_{60} in various solvents [25–27], a few high-impact works were devoted to the partitioning of C_{60} and its derivatives at the water/bilayer interface [21, 28]. Density functional theory (DFT) was applied to probe the applicability of fullerenes in photovoltaics and obtaining fundamental understanding of their electronic structures [10, 29–32]. In the meantime, we are not aware of any investigations of the fullerene dissolution process in real time and length scales.

To summarize, even if "reactive" solvents are counted, pristine fullerenes cannot currently be solvated in the same sense as conventional, smaller molecules can be. Unlike oxygens in ozone, carbons in fullerenes are chemically equivalent and, therefore, no permanent electric moment exists. Short-range dispersive attraction in the case of carbon is inferior to that of more electronegative elements, but is strong enough to keep fullerenes in a solid state at ambient conditions. Because of the supramolecular size of fullerene, its introduction into solvent makes the entropic part of solvation free energy, TdS, significantly negative, whereas the enthalpic constituent is never high enough. The time has come to look at dispersion of fullerenes from a new molecular perspective.

In the present work, we introduce an alternative concept of solvating fullerenes using room-temperature ionic liquids (RTILs). Our concept utilizes the genuine high electronic polarizability of fullerenes, as compared to other carbonaceous compounds, and peculiarities of delocalized electron density in organic cations of RTILs. The original evidence of our method's efficiency was obtained from functional density functional theory coupled with a highly accurate hybrid exchange–correlation functional, and large-scale atomistic-precision molecular dynamics (MD) simulations. It follows from our chemical modeling and simulations that a classical "Like Dissolves Like" rule does not hold for the case of fullerene and 1-butyl-3-methylimidazolium tetrafluoroborate.

2 Insights into Non-bonded Fullerene–Ionic Liquid Interactions

In their condensed state, most ionic liquids [33, 34] are very polarizable and there is an electron density transfer between anion and cation [35–37]. We selected one of such RTILs, 1-butyl-3-methylimidazolium tetrafluoroborate, [BMIM][BF$_4$], to demonstrate our new concept. In turn, fullerenes are also known for high dipole polarizability, 80 Å^3 [38], because of unusual electronic structure and icosahedral symmetry. In order to measure the extent of nonadditivity of C$_{60}$-RTIL non-bonded interactions, we employed hybrid density functional theory methodology. We describe an electron density using a high-quality hybrid exchange–correlation functional, omega B97X-D [39]. Within this functional, the exchange energy is combined with the exact energy from Hartree–Fock theory. Furthermore, empirical atom–atom dispersion correction is included, being of vital importance in the case of fullerenes. Hybrid functionals have been shown to bring significantly improved accuracy in the resulting electronic structure of the simulated quantum mechanical systems, and therefore, polarization effects. While many developments, in particular based on the local density approximation, tend to overestimate electron transfer (ET) between nuclei, carefully "trained" hybrid functionals are free of this defect. According to Chai and Head-Gordon, the functional simultaneously yields satisfactory accuracy for thermochemistry, kinetics, and non-covalent interactions. Based on numerous tests, omega B97X-D is superior for non-bonded interactions over previous hybrid functionals [39]. The 6-31G(d) basis set, containing vacant d-orbitals, was used in all computations since this basis set is continually applied to describe a great variety of carbonaceous compounds. Although 6-31G(d) is less comprehensive than Dunning's correlation-consistent basis sets (especially triple, quadruple, and higher order implementations [40]), it provides reasonable accuracy in the case of ground-state systems. Note that implementation of 6-31G(d) instead of aug-cc-PVTZ [40] decreases computational cost of the same hybrid DFT method by at least one order of magnitude.

The system containing one C$_{60}$ and 500 [BMIM][BF$_4$] ion pairs was originally simulated using empirical scaled-charge potential for [BMIM][BF$_4$], introduced by one of us earlier [35]. The C$_{60}$ fullerene was represented by suitable AMBER-type Lennard–Jones (12, 6), LJ, carbon parameters [41]. The set of empirical parameters for C$_{60}$ and [BMIM][BF$_4$] is listed in Ref. [42] After equilibrium had been reached at 300 K, we extracted coordinates of C$_{60}$ with its solvation shells. Solvation shells within the radius of 0.8 (five ion pairs), 1.0 (ten ion pairs), 1.2 (24 ion pairs), and 1.4 nm (34 ion pairs), Fig. 1, were generated. C$_{60}$ in contact with a single ion pair was used for comparison. Binding energy, corresponding to non-bonded interactions in each shell, electron localization, and full orbital structure were calculated using omega B97X-D/6-31G(d). Basis set superposition error (ca. 20 % of average binding energy) was removed using the counterpoise

Fig. 1 The first solvation shells of fullerene. All ions of the shell are within 0.8 (**a**), 1.0 (**b**), 1.2 (**c**), and 1.4 nm (**d**) from C_{60}. The geometries of configurations have been optimized using hydrid DFT (see methodology)
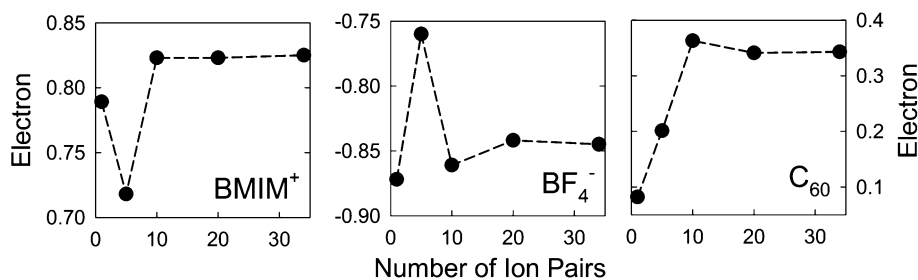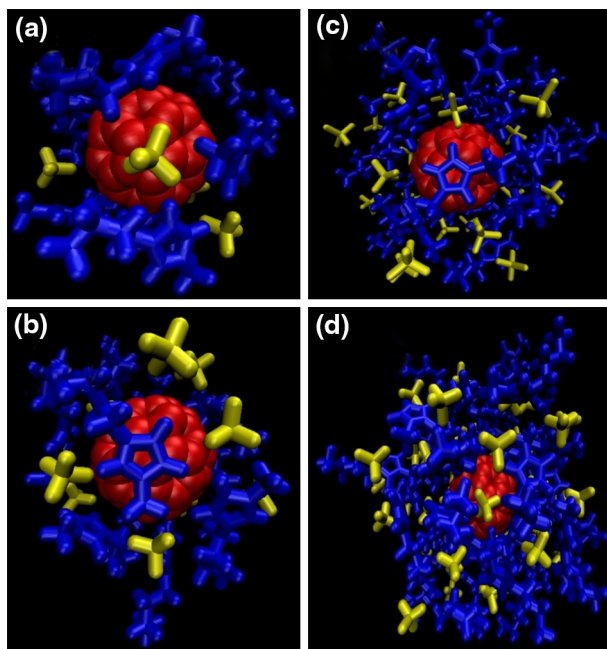
Fig. 2 Electron charge on cation (BMIM$^+$), anion (BF$_4^-$), and fullerene (C_{60}) as a function of the number of ion pairs

technique. Figure 2 suggests that some electron transfer indeed occurs between ions and C_{60}. Brought into direct non-bonded contact with the RTIL, fullerene lost a fraction of electron density, resulting in the +0.35e charge. The depicted charges were obtained using real-space integration of electron density within certain radius from the nucleus, based on the classical Hirshfeld technique. The total electron charge on C_{60} stabilizes after the number of ions achieves the size of the fullerene first solvation shell. Additional increase of the shell size does not lead to any alteration of the electron transfer phenomenon. The binding energies (Fig. 3) between C_{60} and RTIL suggested by the original potential (essentially based on the Lorenz–Berthelot assumption) appear underestimated by 15–20 %. We correlate this underestimation with the electron transfer discussed above (Fig. 2). The transfer is promoted via disturbance of the fullerene highest energy electrons by an electric field of neighboring ions. However, a complete ionization of C_{60} does not

take place in these systems. Based on the same modeling scheme, the cationization of C_{60} in vacuum costs the system ca. 400 kJ·mol^{-1}, whereas anionization costs ca. 500 kJ·mol^{-1}. Since the observed non-additive interaction is caused by an induced dipole, it should be described by a specific energetic well depth parameter. Such a parameter can be epsilon in the LJ potential, in contrast to adjustment of permanent Coulombic charges on the C_{60} and ions. Using an iterative procedure, we altered epsilons for pairwise C_{60}-$BMIM^+$ and C_{60}-BF_4^- interactions. An optimal set of parameters to approximate non-bonded energetics, predicted by DFT, was generated (Fig. 3). Note, that well depth parameters were changed uniformly, irrespective of the nature of each chemical element. It is an obvious approximation, justified by the fact that all involved atoms are of similar size and therefore exhibit similar polarizabilities. Pairwise epsilons were changed only for polar moieties of RTIL. The workability of this approximation to accurately describe (Fig. 3) binding in the case of each of the five shells is a key evidence in favor of our methodological solution. After the refinement of the force field, the MD system was additionally equilibrated, new solvation shells were produced, and DFT calculations were repeated. However, the resulting binding energies are nearly the same as in the initial case. The solvation shell structures and ion orientations near the fullerene surface remained intact.

According to the snapshots in Fig. 1, C_{60} is preferentially coordinated by cations. Interestingly, cations coordinate C_{60} by their polar moiety, the imidazole ring, and not by the hydrophobic –CH_2–CH_2–CH_2–CH_3 chain. The qualitative observations are the same, irrespective of using original FF or refined FF. This orientation is more preferable for a periodic system due to relatively strong dispersion-type attraction between nitrogen atoms of the imidazole ring and carbon atoms of fullerene. Although RTIL imposes certain polarization on C_{60}, no *chemical bonding* occurs between these particles. In the case of the first solvation shell (ten ions pairs), the binding energy is 30 kJ·mol^{-1} at 300 K per one [BMIM][BF_4] ion pair. Being normalized per number of atoms in the polar part of cation and anion, it is weaker than conventional hydrogen bonding. A few highest energy π-orbitals of C_{60} are responsible for the observed electron transfer. Figures 2 and 3 predict that 0.1–0.35e are transferred from fullerene to anion (i.e. to more electronegative fluorine atoms). Noteworthy, the second solvation shell (see values corresponding to 24 and 34 ion pairs) does not contribute to electron transfer. In turn, the number of ions in the first solvation shell plays a major role (see values corresponding to one, five, and ten ions pairs). It would be instructive in future investigations to gain insights about charge transfer dynamics and extend studies to another temperature range, since electronic polarization is known to depend on temperature. An important example of such a study is provided in Ref. [43]. Remarkably, solvation leads to an energy increase by 0.1–0.3 eV (depending on the shell size) of the highest occupied and the lowest unoccupied orbitals, localized on fullerene. Such significant shift normally indicates a strong coupling between the solute and the solvent.

3 Insights from Large-Scale Molecular Dynamics

A solid species of the C_{60} fullerene was immersed into liquid 1-butyl-3-methylimidazolium tetrafluoroborate (1,500 ion pairs), Fig. 4. Non-equilibrium molecular dynamics was simulated at 300, 310, 320, 350, and 400 K under ambient pressure, until the systems came to thermodynamic equilibrium. Equilibrium properties were derived using 30 ns long trajectories with a time-step of 0.002 ps and coordinates saving frequency of 20,000 frames per nanosecond. Velocity rescaling thermostat [44] and Parrinello–Rahman barostat [45] with coupling constants of 1.0 and 4.0 ps were turned on to represent NPT ensembles of

Fig. 3 Binding energy between C_{60} and [BMIM][BF$_4$] as a function of the number of ion pairs: **a** normalized per mole of fullerenes; **b** normalized per mole of [BMIM][BF$_4$]; **c** percentage difference between original and refined models. Original model is *red circles*, DFT energy is *green circles*, refined model is *blue triangles* (Color figure online)
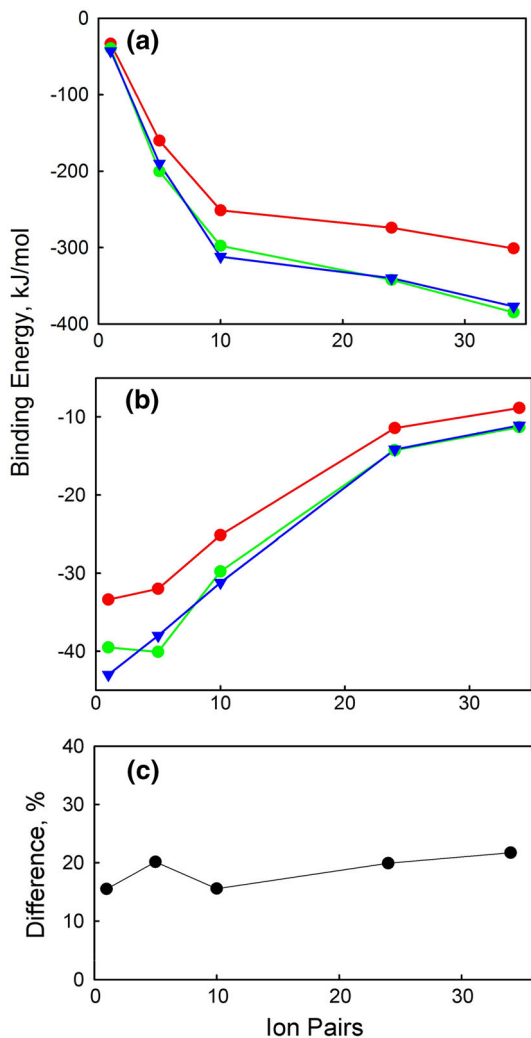

these systems. Covalent bonds of heavy elements with hydrogen atom were constrained using the LINCS algorithm [46], which allows for integration time-step increase without influencing computational stability. The force field was refined as described above. Note, that our model provides average C_{60}-RTIL and RTIL–RTIL energetics ideally concordant with average energetics from the hybrid density functional theory method. The Lennard–Jones interactions were gradually shifted to zero between 1.2 and 1.3 nm. The real-space Coulomb interactions were truncated at 1.4 nm. Their long-range parts were taken into account via the particle-mesh Ewald method [47]. All large-scale simulations were carried out using the GROMACS4 software package [48–51].

Fullerene C_{60} is nearly insoluble at 300 K. Although the well-ordered periodic structure of the solid phase changes to cluster-like (Fig. 4), no fullerene is present in the dissolved state (Fig. 5) for a significant time during 300 ns of the spontaneous evolution of the MD system. This result is in excellent agreement with recent experimental observations [52],

Fig. 4 Representative configuration snapshots of the solid (*left*) and dissolved (*right*) state of C_{60}
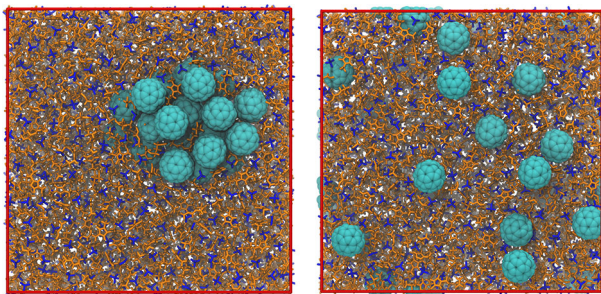
where a few popular RTILs were probed for the C_{70} solvation at room temperature. None of the RTILs, such as 1-butyl-2,3-dimethylimidazolium bis(trifluoromethylsulfonyl)imide, 1-methyl-3-octylimidazolium tetrafluoroborate, 1-methyl-3-octylimidazolium hexafluorophosphate, 1-methyl-3-octylimidazolium bis(trifluoromethylsulfonyl)imide, 1-decyl-3-methylimidazolium tetrafluoroborate, methyltrioctylammonium bis(trifluoromethylsulfonyl)imide, trihexyltetradecylphosphonium chloride, etc., appeared to be an efficient solvent for fullerene, according to fluorescent measurements reported by Martins et al. [53]. However, some of the above RTILs demonstrated better solvation of C_{70} as compared to [BMIM][BF$_4$], from 0.02 up to 0.06 g·L^{-1}. Unfortunately, all cited values are nearly negligible.

Despite failure at ambient conditions, the simulated RTIL, [BMIM][BF$_4$], becomes outstandingly successful as a solvent upon just 20 K temperature increase, 5 g·L^{-1} (310 K), 49 g·L^{-1} (320 K), >66 g·L^{-1} (333 K). Since the enthalpic factor does not change significantly between 300 and 320 K [9], the dissolution is boosted due to an entropic factor increase. We were unable to identify *maximum* C_{60} solubility at higher temperatures, since the originally scheduled systems contained only 30 fullerene molecules corresponding to a maximum solubility of 66 g·L^{-1}. This limit was achieved and exceeded at 333 K. Compare 66 g·L^{-1} to the solubility potential of "reactive" solvents [14]. No reaction between C_{60} and RTIL occurs in our case.

The above findings look very encouraging and motivated us to take a closer look at the representatives of other families of RTILs in order to foster solubility towards ever higher values. Mutual polarization of [BMIM][BF$_4$] and C_{60} plays a key role in successful dissolution. The ionic nature of the [BMIM][BF$_4$] liquid and delocalized charge on the cation are important prerequisites for their electronic polarizability. The elaborated approach is possible only with RTILs, but impossible with solutions of ions in *polar* molecular liquids. In the latter case, ions are strongly solvated by the solvent molecules and cannot approach the fullerene. The fullerene is surrounded predominantly by neutral particles, which, in most cases, exhibit insignificant (e.g. alcohols) to negligible (e.g. nitriles) polarization potential.

Figure 5 depicts radial distribution functions between fullerene center-of-masses. Undissolved cluster at 300 K (Fig. 4) is evidenced by sharp, well-ordered peaks. The arrangement of peaks in not ideal though, as it is observed at lower temperatures, below 260 K (not shown). Therefore, [BMIM][BF$_4$] exhibits a strong potential for breaking the C_{60}–C_{60} weak bonds even at ambient conditions, and insignificant changes of entropic or enthalpic factors can alter the solvation behavior drastically. It happens at higher temperatures (e.g. 320–333 K), resulting in the unexpectedly high value of minimum 66 g·L^{-1}. Larger clusters of C_{60} must be simulated at $T > 333$ K to tabulate solubility. On
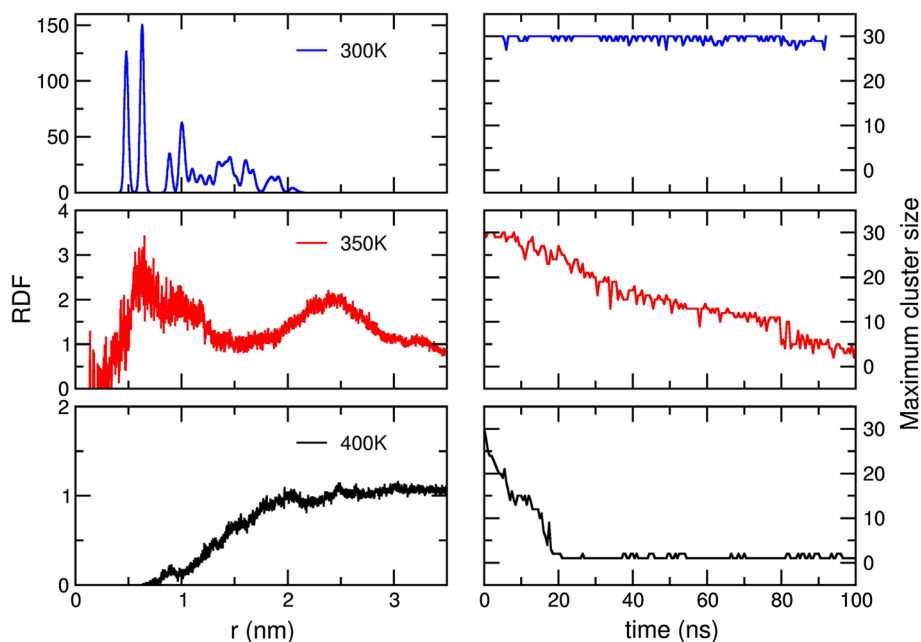
Fig. 5 (*left*) Radial distribution function of the center of mass of fullerenes; (*right*) evolution of the largest cluster size versus simulation time

a related note, Li and co-workers have recently conducted Raman and IR measurements, as well as DFT calculations, to investigate the dispersion of single-walled carbon nanotubes in imidazolium-based ionic liquids at room temperature [53]. On the contrary to their expectations, all methods unequivocally suggested no strong interaction, such as π–π, between carbon nanotubes and imidazolium cations. The only recorded interactions were weak van der Waals attraction, indicating that RTILs are promising solvents to disperse nanotubes without influencing their electronic structure and properties.

The distance of 0.8 nm defines the first coordination sphere of the cluster at 300 K (Fig. 5, left). The neighboring fullerene molecules are considered aggregated when the distance between their centers does not exceed 0.8 nm. With this information in mind, it was possible to analyze the time evolution of the dissolution process in terms of the size of the largest cluster (Fig. 5, right). The dissolution process takes ca. 20 ns at 400 K and ca. 100 ns at 350 K. The dissolution time/speed depends on the volume of the solid phase and on interface surface. With the above data from MD simulations, the speed of C_{60} solvation can be assessed for various aggregate sizes and various external conditions. Statistics of the cluster sizes (Fig. 6), accumulated during an equilibrium stage of simulation, clearly illustrates that dissolution takes place. This process is thermodynamically favorable. Interestingly, a few C_{60} dimers and trimers are recorded in [BMIM][BF$_4$], although their fractions do not exceed 10 %. Such dimers and trimers are wide-spread in the aqueous and nonaqueous electrolyte solutions.

It should be underlined that our observations break one of the most solid rules in chemistry, the "Like Dissolves Like" rule. This statement indicates that a solute will dissolve best in a solvent that has a similar chemical structure to itself. The solvation capacity of a solvent depends primarily on its polarity, i.e. dipole moment. For instance, a
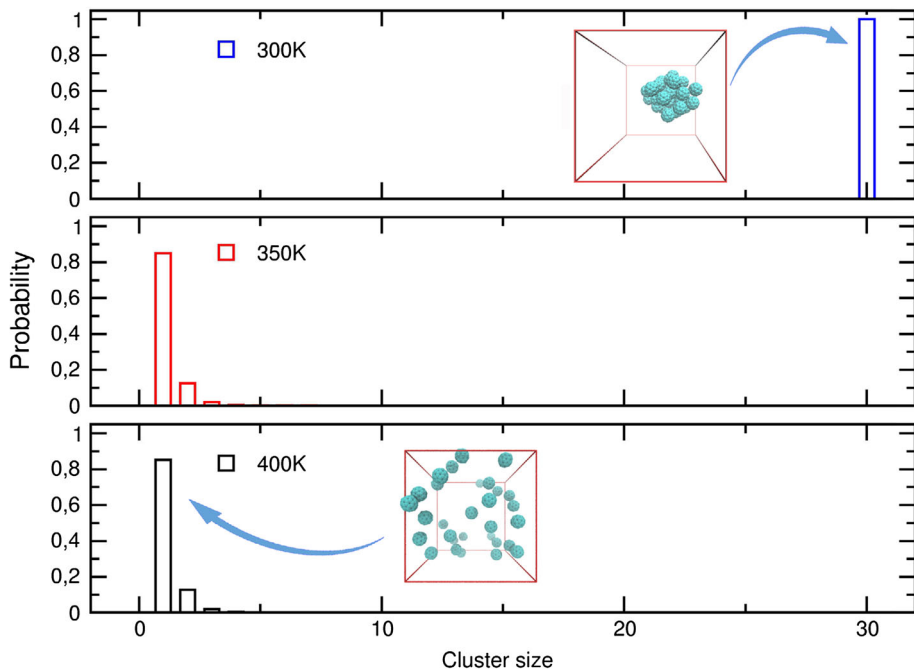
Fig. 6 Cluster size distributions of C_{60} in [BMIM][BF$_4$] at 300, 350, and 400 K. Although all fullerenes belong to the same cluster at 300 K, a variety of aggregates (monomers, dimers, trimers) are observed at higher temperatures

hydrophilic solute, such as sodium sulfate, is soluble in polar water, less soluble in fairly polar ethanol, and insoluble in all non-polar solvents such as benzene. In contrast, a hydrophobic solute, such as naphthalene, is insoluble in water, fairly soluble in ethanol, and soluble in non-polar benzene. The fullerenes are well-known as highly hydrophobic solutes, whereas 1-butyl-3-methylimidazolium tetrafluoroborate is a polar ionic compound. According to the rule, they should not form a single phase, but in practice they form quite a concentrated solution, thanks to the electron transfer phenomenon. One can rephrase that [BMIM][BF$_4$] lowers the hydrophobicity of C_{60} after they mix.

4 Ionic Liquids Versus Molecular Liquids

In order to generalize our findings, we performed an additional investigation of the electron transfer effect for a set of ionic liquids, representing four families. The solvation shells, consisting of *N*-butylpyridinium chloride ([BPY][Cl]), ethylammonium bis(trifluorome-thane)sulfonamide ([Et$_4$N][TFSI]), ethylphosphonium tetrafluoroborate ([Et$_4$P][BF$_4$]), and 1-methyl-3-ethylimidazolium hexafluorophosphate ([EMIM][PF$_6$]), were considered using the methodology introduced above. The obtained results were compared to a range of popular molecular solvents, such as ethanol, acetonitrile, dimethyl sulfoxide (DMSO), cyclohexane, 1,2,4-trimethylbenzene, and chloroform, whose modest to average perfor-mance for C_{60}/C_{70} dispersion had been already documented [12]. The electron transfer in each system is summarized in Table 1. According to hybrid DFT, C_{60} exists as a partially

Table 1 Electron transfer (in electron charge units) from C_{60} fullerene to its solvation shell formed by ionic and molecular solvents, computed using hybrid density functional theory at the omega B97XD/6-31G(d) level

Ionic liquid	Electron transfer (e)	Molecular liquid	Electron transfer (e)
[EMIM][PF$_6$]	0.18	Ethanol	0.06
[Et$_4$N][TFSI]	0.09	Acetonitrile	0.01
[Et$_4$P][BF$_4$]	0.01	DMSO	0.07
[BPY][Cl]	**0.47**	Chloroform	0.23
[BMIM][BF$_4$]	**0.35**	Cyclohexane	0.16
		1,2,4-Trimethylbenzene	0.08
		Water	0.27

Bold values indicate largest amount of electron density transfer

The electron transfer occurs from high-energy π-orbitals of fullerene to ionic or molecular solvent in all presented systems

charged particle in nearly all solutions. The absolute value of total charge on C_{60} varies from 0.01 e (acetonitrile and [Et$_4$N][BF$_4$]) to 0.47 e ([BPY][Cl]). We did not find a clear correspondence between polarity (dipole moment) of the solvent and total charge on the C_{60}. For instance, acetonitrile possesses a significant dipole moment (3.9 D), but it imposes a negligible total charge on C_{60}. In turn, the dipole moment of the [BPY][Cl] ion pair is large, 6.12 D (computed value). Cyclohexane is non-polar, does not contain either strongly electronegative elements or aromatic moieties, nevertheless ET equals 0.16. We suppose that ET can be numerically correlated with HOMO and LUMO energy levels in combination with localization of these orbitals. The hypothesis needs more comprehensive elaboration with a synergetic application of ab initio modeling and spectroscopic experiments.

Ammonium and phosphonium RTILs do not polarize C_{60}, irrespective of the anion. The most intuitive explanation is that positive charge on the cations is deeply buried and is chemically inactive. Interestingly, anions do not impose any effect on the fullerene in these two cases. However, a transfer of 0.35 e was recorded when tetrafluoroborate is coupled with an imidazolium cation.

Among molecular solvents, water and chloroform exhibit the largest ETs, 0.27 and 0.23, respectively. Both liquids are polar solvents, μ(H$_2$O) = 1.85 D, μ(CHCl$_3$) = 1.04 D, with a significant degree of dipole–dipole interactions determining their molecular structures in the condensed phase. The van der Waals interactions are not decisive in chloroform and marginal is water. Despite the derived ET, these solvents cannot be efficient for fullerenes. This conclusion is well supported by direct experiments on solubilization [12]. Thus far, the electron transfer effect was not included in computer simulations of C_{60} dispersibility in the liquid phases, since it was assumed insignificant. Accounting for ET in future must help to achieve better description of structure and transport properties of the mentioned systems.

1,2,4-Trimethylbenzene was reported as a relatively successful solvent before (even better than benzene) [12], but the computed ET is a few times smaller than that of pyridinium and imidazolium RTILs (Table 1). The good solvation ability of 1,2,4-trimethylbenzene probably comes mainly from entropic contribution to the solvation free energy and not from the electronic polarization.

Solvation is observed everywhere in nature. Most of chemical reactions occur in solutions. This is an extremely complicated process involving a number of independent and

semi-independent factors, such as strength of dipole–dipole interactions, π–π interactions, weak dispersion interactions, hydrogen bonding, molecular and ionic shapes, conformational flexibility, potential energy surfaces, ability of solute to dissociate, mass and electron densities, temperature, external pressure, etc. These factors are classically divided into entropic and enthalpic contributions. In this work, we deliberately tuned only the second contribution. We theoretically unveil that C_{60} exists as a partially charged particle in many solutions. This phenomenon can be employed to engineer more efficient solvents for fullerenes, since obtaining a real solution of this compound is of significant interest for many fundamental and applied areas.

5 Conclusions

To recapitulate, an alternative approach to increase dispersion of C_{60} molecules was outlined in the present work. Although a zero solubility in [BMIM][BF$_4$] was recorded at 300 K (in perfect agreement with experimental observations [52]), the calculated solubility increases drastically with temperature: S (310 K) = 5 g·L^{-1}, S (320 K) = 49 g·L^{-1}, S (333 K) > 66 g·L^{-1}. The accuracy of the results is justified by carefully parameterized non-bonded interactions among all components in the simulated system based on electronic structure calculations. Although our atomistic-precision MD study cannot compete with an all-electron description in accuracy, it is the only computationally feasible approach to derive insights for the appropriate time (over 300 ns) and length (over 500 nm^3) scales.

Here, we chose [BMIM][BF$_4$] as an exemplary RTIL due to its wide availability and use in fundamental research and technology [35, 37, 52, 54]. We suppose that certain other RTILs can exhibit competitive affinity towards fullerene (enthalpic factor). As fullerene exhibits π-stacking with aromatic compounds, one can hypothesize that polyaromatic cations, such as isoquinolinium$^+$, isothiouronium$^+$, and triphenylphosphonium$^+$ may be decent solvents. In the latter case, both electronic polarization and π-stacking are involved in the intermolecular binding. Unfortunately, we currently do not possess trustworthy information about liquid ranges of these novel compounds.

Trace admixtures of salts containing alkali ions, such as Li$^+$, Na$^+$, K$^+$, may improve solubility, provided that small, mobile cations localize near the C_{60} surface or penetrate inside the cavity. Previous study suggested that even a single lithium atom inside C_{60} greatly perturbs the electronic energy levels of the whole structure [10]. Experimental studies on well-dispersed C_{60} molecules in [BMIM][BF$_4$] and other mentioned RTILs upon a wide temperature range are of large fundamental interest.

References

1. Kroto, H.W., Heath, J.R., Obrien, S.C., Curl, R.F., Smalley, R.E.: C-60—buckminsterfullerene. Nature **318**, 162–163 (1985)
2. Yannoni, C.S., Hoinkis, M., Devries, M.S., Bethune, D.S., Salem, J.R., Crowder, M.S., Johnson, R.D.: Scandium clusters in fullerene cages. Science **256**, 1191–1192 (1992)
3. Theobald, J.A., Oxtoby, N.S., Phillips, M.A., Champness, N.R., Beton, P.H.: Controlling molecular deposition and layer structure with supramolecular surface assemblies. Nature **424**, 1029–1031 (2003)

4. Mchedlov-Petrossyan, N.O.: Fullerenes in molecular liquids. Solutions in "good" solvents: another view. J. Mol. Liq. **161**, 1–12 (2011)

5. Bernardi, M., Lohrman, J., Kumar, P.V., Kirkeminde, A., Ferralis, N., Grossman, J.C., Ren, S.Q.: Nanocarbon-based photovoltaics. ACS Nano **6**, 8896–8903 (2012)

6. Schmidt-Hansberg, B., Sanyal, M., Klein, M.F.G., Pfaff, M., Schnabel, N., Jaiser, S., Vorobiev, A., Muller, E., Colsmann, A., Scharfer, P., Gerthsen, D., Lemmer, U., Barrena, E., Schabel, W.: Moving through the phase diagram: morphology formation in solution cast polymer–fullerene blend films for organic solar cells. ACS Nano **5**, 8579–8590 (2011)

7. Chamberlain, T.W., Popov, A.M., Knizhnik, A.A., Samoilov, G.E., Khlobystov, A.N.: The role of molecular clusters in the filling of carbon nanotubes. ACS Nano **4**, 5203–5210 (2010)

8. Corley, D.A., He, T., Tour, J.M.: Two-terminal molecular memories from solution-deposited C-60 films in vertical silicon nanogaps. ACS Nano **4**, 1879–1888 (2010)

9. Ruoff, R.S., Malhotra, R., Huestis, D.L., Tse, D.S., Lorents, D.C.: Anomalous solubility behavior of C60. Nature **362**, 140–141 (1993)

10. Chaban, V.V., Prezhdo, V.V., Prezhdo, O.V.: Covalent linking greatly enhances photoinduced electron transfer in fullerene–quantum dot nanocomposites: time-domain ab initio study. J. Phys. Chem. Lett. **4**, 1–6 (2013)

11. Semenov, K.N., Charykov, N.A.: Temperature dependence of solubility of individual light fullerenes and industrial fullerene mixture in 1-chloronaphthalene and 1-bromonaphthalene. J. Chem. Eng. Data **55**, 2373–2378 (2010)

12. Semenov, K.N., Charykov, N.A., Keskinov, V.A., Piartman, A.K., Blokhin, A.A., Kopyrin, A.A.: Solubility of light fullerenes in organic solvents. J. Chem. Eng. Data **55**, 13–36 (2010)

13. Scrivens, W.A., Tour, J.M.: Potent solvents for C-60 and their utility for the rapid acquisition of C-13 nmr data for fullerenes. J. Chem. Soc. Chem. Commun. **15**, 1207–1209 (1993)

14. Talukdar, S., Pradhan, P., Banerji, A.: Electron donor-acceptor interactions of C-60 with n- and pi-donors: a rational approach towards its solubility. Fuller. Sci. Technol. **5**, 547–557 (1997)

15. Lozano, K., Chibante, L.P.F., Sheng, X.Y., Gaspar-Rosas, A., Barrera, E.V.: Physical examination and handling of wet and dry C60. In: Battle, T.P., Henein, H. (eds.) Processing and Handling of Powders and Dusts. Minerals, Metals, and Materials Society, Mexico (1997)

16. Pourbasheer, E., Riahi, S., Ganjali, M.R., Norouzi, P.: Prediction of solubility of fullerene C-60 in various organic solvents by genetic algorithm-multiple linear regression. Fuller. Nanotub. Carb. Nanostruct. **19**, 585–598 (2011)

17. Furuishi, T., Ohmachi, Y., Fukami, T., Nagase, H., Suzuki, T., Endo, T., Ueda, H., Tomono, K.: Enhanced solubility of fullerene (C(60)) in water by inclusion complexation with cyclomaltononaose (delta-CD) using a cogrinding method. J. Incl. Phenom. Macrocycl. Chem. **67**, 233–239 (2010)

18. Troshin, P.A., Susarova, D.K., Khakina, E.A., Goryachev, A.A., Borshchev, O.V., Ponomarenko, S.A., Razumov, V.F., Sariciftci, N.S.: Material solubility and molecular compatibility effects in the design of fullerene/polymer composites for organic bulk heterojunction solar cells. J. Mater. Chem. **22**, 18433–18441 (2012)

19. Monticelli, L.: On atomistic and coarse-grained models for C-60 fullerene. J. Chem. Theory Comput. **8**, 1370–1378 (2012)

20. Qian, H.J., van Duin, A.C.T., Morokuma, K., Irle, S.: Reactive molecular dynamics simulation of fullerene combustion synthesis: Reaxff versus DFTB potentials. J. Chem. Theory Comput. **7**, 2040–2048 (2011)

21. Qiao, R., Roberts, A.P., Mount, A.S., Klaine, S.J., Ke, P.C.: Translocation of C-60 and its derivatives across a lipid bilayer. Nano Lett. **7**, 614–619 (2007)

22. Chiu, C.C., DeVane, R., Klein, M.L., Shinoda, W., Moore, P.B., Nielsen, S.O.: Coarse-grained potential models for phenyl-based molecules: II. Application to fullerenes. J. Phys. Chem. B **114**, 6394–6400 (2010)

23. Monticelli, L., Salonen, E., Ke, P.C., Vattulainen, I.: Effects of carbon nanoparticles on lipid membranes: a molecular simulation perspective. Soft Matter **5**, 4433–4445 (2009)

24. Monticelli, L., Kandasamy, S.K., Periole, X., Larson, R.G., Tieleman, D.P., Marrink, S.J.: The MARTINI coarse-grained force field: extension to proteins. J. Chem. Theory Comput. **4**, 819–834 (2008)

25. Maciel, C., Fileti, E.E., Rivelino, R.: Assessing the solvation mechanism of C-60(OH)(24) in aqueous solution. Chem. Phys. Lett. **507**, 244–247 (2011)

26. Colherinhas, G., Fonseca, T.L., Fileti, E.E.: Theoretical analysis of the hydration of C-60 in normal and supercritical conditions. Carbon **49**, 187–192 (2011)

27. Malaspina, T., Fileti, E.E., Rivelino, R.: Structure and UV-Vis spectrum of C-60 fullerene in ethanol: a sequential molecular dynamics/quantum mechanics study. J. Phys. Chem. B **111**, 11935–11939 (2007)

28. Wong-Ekkabut, J., Baoukina, S., Triampo, W., Tang, I.M., Tieleman, D.P., Monticelli, L.: Computer simulation study of fullerene translocation through lipid membranes. Nat. Nanotechnol. **3**, 363–368 (2008)

29. Lopez, V., Roman-Perez, G., Arregui, A., Mateo-Marti, E., Banares, L., Martin-Gago, J.A., Soler, J.M., Gomez-Herrero, J., Zamora, F.: Azafullerene-like nanosized clusters. ACS Nano **3**, 3352–3357 (2009)

30. Ge, L., Jefferson, J.H., Montanari, B., Harrison, N.M., Pettifor, D.G., Briggs, G.A.D.: Effects of doping on electronic structure and correlations in carbon peapods. ACS Nano **3**, 1069–1076 (2009)

31. Shukla, M.K., Dubey, M., Leszczynski, J.: Theoretical investigation of electronic structures and propertiesof C-60-gold nanocontacts. ACS Nano **2**, 227–234 (2008)

32. Zheng, G.S., Irle, S., Elstner, M., Morokuma, K.: Quantum chemical molecular dynamics model study of fullerene formation from open-ended carbon nanotubes. J. Phys. Chem. A **108**, 3182–3194 (2004)

33. Lopes, J.N.C., Padua, A.A.H.: CL&P: a generic and systematic force field for ionic liquids modeling. Theor. Chem. Acc. **131**, 1129 (2012)

34. Tariq, M., Freire, M.G., Saramago, B., Coutinho, J.A.P., Lopes, J.N.C., Rebelo, L.P.N.: Surface tension of ionic liquids and ionic liquid solutions. Chem. Soc. Rev. **41**, 829–868 (2012)

35. Chaban, V.V., Voroshylova, I.V., Kalugin, O.N.: A new force field model for the simulation of transport properties of imidazolium-based ionic liquids. Phys. Chem. Chem. Phys. **13**, 7910–7920 (2011)

36. Chaban, V.: Polarizability versus mobility: atomistic force field for ionic liquids. Phys. Chem. Chem. Phys. **13**, 16055–16062 (2011)

37. Chaban, V.V., Prezhdo, O.V.: A new force field model of 1-butyl-3-methylimidazolium tetrafluoroborate ionic liquid and acetonitrile mixtures. Phys. Chem. Chem. Phys. **13**, 19345–19354 (2011)

38. Perpete, E.A., Champagne, B., Kirtman, B.: Large vibrational nonlinear optical properties of C-60: a combined Hartree–Fock/density-functional approach. Phys. Rev. B **61**, 13137–13143 (2000)

39. Chai, J.D., Head-Gordon, M.: Long-range corrected hybrid density functionals with damped atom–atom dispersion corrections. Phys. Chem. Chem. Phys. **10**, 6615–6620 (2008)

40. Davidson, E.R.: Comment on Dunning's correlation-consistent basis sets—comment. Chem. Phys. Lett. **260**, 514–518 (1996)

41. Rivelino, R., Maniero, A.M., Prudente, F.V., Costa, L.S.: Theoretical calculations of the structure and UV–Vis absorption spectra of hydrated C-60 fullerene. Carbon **44**, 2925–2930 (2006)

42. Maciel, C., Fileti, E.E.: Molecular interactions between fullerene C-60 and ionic liquids. Chem. Phys. Lett. **568**, 75–79 (2013)

43. Sawada, H., Kasai, R.: Solubilization of fullerene into ionic liquids by the use of fluoroalkyl end-capped oligomers. Polym. Adv. Technol. **16**, 655–658 (2005)

44. Bussi, G., Donadio, D., Parrinello, M.: Canonical sampling through velocity rescaling. J. Chem. Phys. **126**, 014101 (2007)

45. Parrinello, M., Rahman, A.: Polymorphic transitions in single-crystals—a new molecular-dynamics method. J. Appl. Phys. **52**, 7182–7190 (1981)

46. Hess, B., Bekker, H., Berendsen, H.J.C., Fraaije, J.G.E.M.: LINCS: a linear constraint solver for molecular simulations. J. Comput. Chem. **18**, 1463–1472 (1997)

47. Darden, T., York, D., Pedersen, L.: Particle mesh Ewald—an N. Log(N) method for Ewald sums in large systems. J. Chem. Phys. **98**, 10089–10092 (1993)

48. van der Spoel, D., Hess, B.: GROMACS-the road ahead. Wiley Interdiscip. Rev. **1**, 710–715 (2011)

49. Hess, B., Kutzner, C., van der Spoel, D., Lindahl, E.: GROMACS 4: algorithms for highly efficient, load-balanced, and scalable molecular simulation. J. Chem. Theory Comput. **4**, 435–447 (2008)

50. Van der Spoel, D., Lindahl, E., Hess, B., Groenhof, G., Mark, A.E., Berendsen, H.J.C.: GROMACS: fast, flexible, and free. J. Comput. Chem. **26**, 1701–1718 (2005)

51. Lindahl, E., Hess, B., van der Spoel, D.: GROMACS 3.0: a package for molecular simulation and trajectory analysis. J. Mol. Model. **7**, 306–317 (2001)

52. Martins, S., Fedorov, A., Afonso, C.A.M., Baleizao, C., Berberan-Santos, M.N.: Fluorescence of fullerene C-70 in ionic liquids. Chem. Phys. Lett. **497**, 43–47 (2010)

53. Wang, J.Y., Chu, H.B., Li, Y.: Why single-walled carbon nanotubes can be dispersed in imidazolium-based ionic liquids. ACS Nano **2**, 2540–2546 (2008)

54. Hantal, G., Voroshylova, I., Cordeiro, M.N.D.S., Jorge, M.: A systematic molecular simulation study of ionic liquid surfaces using intrinsic analysis methods. Phys. Chem. Chem. Phys. **14**, 5200–5213 (2012)